Stratosphere-troposphere exchange of mass and ozone

Mark A. Olsen
Goddard Earth Sciences and Technology Center, University of Maryland Baltimore County, Baltimore, Maryland, USA

Mark R. Schoeberl and Anne R. Douglass
NASA Goddard Space Flight Center, Greenbelt, Maryland, USA

Received 1 July 2004; revised 12 October 2004; accepted 29 October 2004; published 31 December 2004.

[1] This study examines the relationship between the extratropical cross-tropopause fluxes of mass and ozone. The adiabatic and diabatic components of the net fluxes are also compared. The rate of change of mass in the lowermost stratosphere and the flux across the 380 K isentropic surface are used to determine the net tropopause mass flux in the framework of a global circulation model. The diabatic mass flux is calculated from the heating rate at the tropopause, and the adiabatic component is determined by the difference of the net and diabatic fluxes. Consistent ozone fields are obtained by driving the Goddard Chemistry and Transport Model with meteorological output of the global circulation model for the same years. The ozone flux is determined by convolving the mass flux and ozone mixing ratio. The results show the following: (1) The seasonal cycle of the ozone mixing ratio is out of phase with the transport cycle leading to a temporal offset of the mass and ozone fluxes; (2) the downward net diabatic flux of mass and ozone occurs primarily at middle latitudes while the adiabatic mass flux is dominated by troposphere-to-stratosphere transport at higher latitudes; and (3) the Southern Hemisphere stratospheric vortex is more effective at blocking meridional transport, resulting in a phase difference of mean tropopause ozone mixing ratio in the higher Southern Hemisphere latitudes with respect to the corresponding Northern Hemisphere season and location. Finally, this study suggests that individual pathways of cross-tropopause transport are unlikely to be the result of simultaneous adiabatic and diabatic mechanisms. *INDEX TERMS:* 0341 Atmospheric Composition and Structure: Middle atmosphere—constituent transport and chemistry (3334); 3362 Meteorology and Atmospheric Dynamics: Stratosphere/troposphere interactions; 3319 Meteorology and Atmospheric Dynamics: General circulation; *KEYWORDS:* stratosphere-troposphere exchange, ozone transport, mass transport

Citation: Olsen, M. A., M. R. Schoeberl, and A. R. Douglass (2004), Stratosphere-troposphere exchange of mass and ozone, *J. Geophys. Res.*, *109*, D24114, doi:10.1029/2004JD005186.

1. Introduction

[2] The transport of mass and chemical constituents from the stratosphere to the troposphere is an important element of many atmospheric chemistry and climate studies. The stratosphere and troposphere present significantly different chemical environments, and the amount of mass and constituents transported between these environments is an important boundary condition in understanding the changing atmosphere. Ozone is one of the constituents important to climate studies since it is a part of the oxidation cycle of the atmosphere [*Levy*, 1971] and is a major greenhouse gas [*Ramanathan et al.*, 1987]. *Roelofs et al.* [1997] have shown that anthropogenic sources have increased and altered the seasonal cycle of the tropospheric ozone burden since preindustrial times. Nonanthropogenic ozone is primarily produced in the stratosphere. An accurate determination of the magnitude and variability of the amount that is transported into the troposphere must be known to characterize the impact human activities have on the past, present, and future climate.

[3] The flux of ozone across the tropopause is determined by both the mass flux and the ozone concentration in the lower stratosphere. Qualitatively, much is known about the stratosphere-troposphere exchange (STE) of mass. The Brewer-Dobson circulation can explain the large-scale exchange between the stratosphere and troposphere [*Brewer*, 1949; *Dobson*, 1956]. Air rises into the stratosphere in the tropics and descends at higher latitudes. This motion is the result of the induced secondary circulation associated with wave dissipation in the stratospheric overworld, the atmosphere above the 380 K isentropic surface [*Hoskins*, 1991; *Holton et al.*, 1995]. The magnitude of the extratropical cross-tropopause transport on a long-term average is ultimately determined by the amount of mass that diabatically descends from the overworld into the lowermost stratosphere, the region between the tropopause and the 380 K potential temperature surface. Greater orographic variability in the Northern Hemisphere (NH)

0148-0227/04/2004JD005186

results in more overworld wave driving [*Haynes et al.*, 1991], and the magnitude of the net mass STE in the NH is greater than in the Southern Hemisphere (SH) [e.g., *Appenzeller et al.*, 1996] (hereinafter referred to as A96). However, the strong seasonal cycle of global STE as first noted by *Staley* [1962] is primarily caused by the vertical movement of the tropopause which is indirectly connected to overworld wave driving. The maximum downward flux of mass and trace gases from the stratosphere occurs in the spring of each hemisphere as the tropopause rises relative to the background. Likewise, a fall minimum in the flux exists as the tropopause moves back downward.

[4] Overworld wave driving and its seasonal variability determine the magnitude of STE. Baroclinic systems such as midlatitude cyclones and other mechanisms act as valves across the tropopause, dictating the spatial distribution of STE. The mechanisms of transport may be classified as either diabatic, adiabatic, or possibly some combination of the two. *Reed and Sanders* [1953] first noted that midlatitude cyclones were a significant source of STE, and *Lamarque and Hess* [1994] and *Rood et al.* [1997] show that diabatic processes in cyclone-induced tropopause folds are important mechanisms for cross-tropopause transport. Convective systems reaching tropopause altitudes can raise the tropopause relative to the background mass [*Matsumoto et al.*, 1982]. *Olsen and Stanford* [2001] show that tropospheric latent heating from condensation can also raise the tropopause. Other studies have focused on isentropic transport. *Dethof et al.* [2000] examine the isentropic cross-tropopause mass transport using contour advection [*Norton*, 1994; *Waugh and Plumb*, 1994]. *Jing et al.* [2004] extend this method to examine the isentropic ozone flux. However, no prior studies have examined the net global ozone flux on the basis of both diabatic and adiabatic transport.

[5] Various methods have been used to obtain quantitative estimates of the magnitude of global mass and ozone STE, producing a wide range of estimates. Some estimates have been made by extrapolation from cyclone case studies [*Lamarque and Hess*, 1994; *Beekmann et al.*, 1997]. Dynamical and spatial differences of extratropical cyclones produce a large range of results with this method. Studies using three-dimensional (3-D) models and assimilation systems have been widely used to examine the global flux characteristics of both mass and ozone [e.g., *Roelofs and Lelieveld*, 1995; *Tie and Hess*, 1997; *Hauglustaine et al.*, 1998; *Lamarque et al.*, 1999]. *McLinden et al.* [2000] and *Roelofs et al.* [2003] illustrate that the cross-tropopause ozone flux results given by different 3-D models can be vastly dissimilar in global and case studies, respectively. Some of the differences can be attributed to resolution, parameterization schemes, etc., but other differences remain unresolved. Various empirical diagnostic methods used also give a wide range of flux estimates [e.g., *Murphy and Fahey*, 1994; *Beekmann et al.*, 1997; *Olsen et al.*, 2003].

[6] The net flux through the tropopause is a small residual of large upward and downward transport quantities. A large amount of transient, "shallow" exchange occurs where mass crosses the tropopause only to return a short time later [e.g., *Stohl et al.*, 2003b; *James et al.*, 2003b]. A96 avoids complications introduced by this shallow, transient flux by determining the magnitude and phase of the net extratropical STE from the flux across the 380 K surface and the rate of change of lowermost stratosphere mass. *Schoeberl* [2004] (hereinafter referred to as S04) extended the A96 algorithm in a manner that separates the diabatic and adiabatic fluxes. S04 used this method to compare and contrast STE estimates using various assimilation systems and models. However, neither the A96 method nor the S04 extension provides explicit spatial information of the net flux.

[7] The present study compares the mass and ozone tropopause flux using the algorithm of S04. The mass flux is evaluated from output of a general circulation model (GCM). The ozone flux is computed by convolving the mass flux with ozone mixing ratios from an off-line 3-D chemistry and transport model driven by the meteorological fields output from the same GCM. Thus both the adiabatic and diabatic flux of ozone across the tropopause are quantified in a manner that is consistent with the meteorological fields used to quantify the mass flux. In addition, because in the chemistry and transport model (CTM) the ozone of stratospheric origin is computed and transported separately from the ozone of tropospheric origin, it is possible to quantify the fluxes of stratospheric and tropospheric ozone separately. The spatial distribution of the STE and patterns of transport are also investigated. This work adopts the nomenclature used recently by members of the Influence of Stratosphere-Troposphere Exchange in a Changing Climate on Atmospheric Transport and Oxidation Capacity project [e.g., *Stohl et al.*, 2003a] to distinguish the direction of transport across the tropopause. Stratosphere-to-troposphere transport (STT) and troposphere-to-stratosphere transport (TST) refers to transport in each direction. "STE" will be reserved for the generalized two-way transport across the tropopause. Section 2 discusses the diagnostic algorithm and models used in this work. The flux results are presented in section 3, and a more detailed discussion is in section 4.

2. Method of Analysis

[8] The net tropopause mass flux (F_{trop}) in each hemisphere can be computed from the rate of change in lowermost stratosphere mass (M) and the diabatic flux across the 380 K surface ($F_{380\text{K}}$) following A96,

$$F_{\text{trop}} = \frac{dM}{dt} + F_{380\text{K}}. \tag{1}$$

The fluxes are positive upward. S04 subdivided F_{trop} into adiabatic and diabatic components ($F_{\text{trop-a}}$ and $F_{\text{trop-d}}$, respectively) so that equation (1) may be written as

$$F_{\text{trop-a}} + F_{\text{trop-d}} = \frac{dM}{dt} + F_{380\text{K}}. \tag{2}$$

The diabatic fluxes, $F_{380\text{K}}$ and $F_{\text{trop-d}}$, are computed from heating rate fields using $-\int(\dot{\theta}/g)(dp/d\theta)dA$ where p is pressure, θ is potential temperature, $\dot{\theta}$ is the diabatic heating rate, and A is the area. $F_{\text{trop-a}}$ is then the difference of F_{trop} and $F_{\text{trop-d}}$. Note that both the net tropopause flux and the adiabatic flux are bulk values with no spatial information. In contrast, the heating rate fields provide spatial information of the diabatic fluxes.

[9] As in S04 the present study uses equation (2) to determine the mass flux across the tropopause. The extratropical tropopause is chosen as the 3.5 potential vorticity unit (PVU) surface (1 PVU = 10^{-6} m^2 K kg^{-1} s^{-1}). *Hoerling et al.* [1991] conclude that this PV value is optimal for coarsely gridded data sets, and an analysis by S04 shows that the altitude of this surface is reasonably close to the tropopause determined by the *World Meteorological Organization* [1986] temperature lapse rate definition of the tropopause. Also following the example of S04, the lowermost stratosphere is defined as the region where the mass between the tropopause and 380 K surface exceeds 30 g cm^{-2}. This criterion provides a reasonable fit to the net zero heating rate line on the 380 K surface. Thus, in the present study, the extratropics are defined as the region poleward of the 30 g cm^{-2} line. This work considers only the flux that occurs in this region.

[10] Equation (1) is also used to derive the net flux of ozone across the tropopause. The flux of ozone across the 380 K surface is determined by convolving the 380 K mass flux with the ozone mixing ratios at every grid point. (The diabatic tropopause flux of ozone is likewise computed.) For ozone the rate of mass change term in (1) implicitly includes the net chemical production or loss in addition to the dynamical factors. We demonstrate that it is reasonable to assume that any change in ozone mass in the lowermost stratosphere is due to transport processes because the photochemical lifetime of ozone in this region is much greater than the residence time. The timescale of residence in the lowermost stratosphere is estimated by $M_{O_3}/F_{380\mathrm{K}(O_3)}$, where M_{O_3} is the annual mean mass of ozone in the lowermost stratosphere, and $F_{380\mathrm{K}(O_3)}$ is the annual flux of ozone across the 380 K surface. This residence timescale is on the order of 100 days in both the NH and SH in the context of this study. Production and loss rates from the Goddard Space Flight Center 2-D model [*Fleming et al.*, 2002] show that the net mean lifetime of ozone poleward of 30° and between 138 and 244 hPa is more than an order of magnitude greater than the residence time. Thus neglecting the net ozone chemistry in the lowermost stratosphere for this STE diagnostic algorithm does not significantly alter the results and conclusions presented here. Note that the diabatic calculations are precise and this approximation is only relevant to the net tropopause and adiabatic fluxes of ozone.

[11] The meteorological fields used in this study are from the NASA Goddard Global Modeling and Assimilation Office finite volume general circulation model (FVGCM). The free-running FVGCM uses the National Center for Atmospheric Research Community Climate Model Version 3 physics package [*Kiehl et al.*, 1998]. The transport is computed by the *Lin and Rood* [1996, 1997] algorithm and has a quasi-Lagrangian vertical coordinate [*Lin*, 1997]. *Douglass et al.* [2003] have shown that the large-scale stratospheric transport is realistic. The residual circulation and age of air have also been shown to be more realistic compared to assimilated data sets [*Schoeberl et al.*, 2003]. The FVGCM is run at a horizontal resolution of 2.5° × 2° in the present study. There are 55 vertical levels from the surface to 0.01 hPa. The diabatic heating rates used in calculating the fluxes are inline FVGCM output. While the results do not correspond to any actual years, the FVGCM run used in this study includes Hadley Centre monthly mean sea surface temperatures of the years 1955–1959 from the Atmospheric Model Intercomparison Project.

[12] The global ozone mixing ratio fields used here are calculated using the NASA Goddard 3-D full CTM [*Douglass et al.*, 2003]. This stratospheric chemistry model is driven off-line using FVGCM output every 6 hours. The CTM has a horizontal resolution of 2.5° × 2° and has 28 vertical levels up to 0.43 hPa. The vertical resolution is ~2 km below 60 hPa and ~3.5 km above. The numerical transport algorithm [*Lin and Rood*, 1996] is the same as used within the FVGCM. The 5 years of the CTM run used in this study include measured emissions of ozone-depleting chemical species from the years 1979 to 1983 as given by *World Meteorological Organization* [2003]; thus less ozone depletion potential exists than in the present-day, particularly within the SH polar stratospheric vortex.

[13] The ozone field of the CTM is reasonable compared to ozonesonde data. The shapes of the zonal mean vertical profiles generally agree well with observations (not shown). The greatest difference in magnitude exists in the SH midlatitude lowermost stratosphere where the CTM ozone is biased high with respect to the sonde data (~0.1 ppmv mean difference at 150 hPa between 40° and 60°S). Comparisons to Total Ozone Mapping Spectrometer total column ozone observations are also reasonable (R. Stolarski, NASA Goddard Space Flight Center, personal communication, 2004). There is almost no bias of the mean total column ozone between 60°S and 60°N. The mean seasonal ozone variability is also well represented as a whole over this region. However, the CTM SH polar region is less representative of observations than the NH. Both the seasonal variability and the magnitude of the total column ozone are slightly too large in the polar SH. The column ozone is ~10% too high throughout the year in this region. However, the development of the Antarctic stratospheric vortex and resulting ozone hole are well represented. In the NH high latitudes the magnitude of the CTM column ozone does not show a significant bias with respect to observations. In the tropics the lack of a quasi-biennial oscillation in the CTM ozone field is the most notable difference from observations. Overall the CTM provides a reasonable representation of the ozone field for the purposes of this study. As will be discussed in section 4, the differences from observations have the greatest impact on the magnitude of the estimated ozone flux in the SH.

[14] The ozone field in the CTM is subdivided into stratospheric origin and tropospheric origin ozone components (hereinafter "stratospheric ozone" and "tropospheric ozone," referring to the region of origin regardless of where it is located later due to transport). The net ozone field is determined by the sum of these two components. Both production and loss of stratospheric ozone are explicitly computed in the stratosphere. The stratospheric ozone that enters the troposphere is subject to a loss rate proportional to the ozone mixing ratio. There is no production of stratospheric ozone below the tropopause. The production and loss of the tropospheric ozone in the troposphere are taken from the Harvard GEOS-CHEM tropospheric chemistry model [*Bey et al.*, 2001]. In the stratosphere, there is no tropospheric ozone production, but the tropospheric ozone is subject to the same photochemical loss as stratospheric

ozone. In this work the sum of the stratospheric and tropospheric components will be referred to as "total ozone" (not to be confused with "total column ozone"). The term "net" will be used for a global sum or a sum of adiabatic and diabatic fluxes depending on context.

[15] The mass and ozone fluxes are computed for 6 days of each month (days 1, 5, 10, 15, 20, and 25) for 5 years. The results for the timescales considered are not altered by the use of 72 days per year. The annual estimates do not significantly change in tests using more days, and the seasonal cycles are well represented. Throughout this work, climatological 5 year means from a continuous 5 year integration are presented and discussed unless otherwise explicitly stated.

3. Results

3.1. 380 K Flux

[16] The 5 year mean annual cycle of mass and ozone flux across the extratropical 380 K surface is shown in Figure 1. Note that the minimum (maximum) downward flux occurs at the highest (lowest) point on each curve. This sign convention is consistent with that used in Figure 2. Since the ozone flux is computed from the convolution of the mass flux with the ozone mixing ratio on the 380 K surface, the seasonal cycle of mean ozone mixing ratio on the 380 K surface alters the shape of the ozone flux compared to the mass flux. In the SH the minimum downward fluxes of mass and ozone nearly coincide in November and December. During the SH summer and spring the downward flux of ozone and mass increase at approximately the same rate until the end of April. At this time the downward mass flux levels off to a maximum before decreasing by the end of June. However, the ozone flux continues to increase at this time and doesn't start significantly decreasing until the end of July. This is caused by the mean ozone mixing ratio of the air transported through the SH extratropical 380 K surface increasing from the end of April through June, whereas it decreases after July.

[17] In contrast to the SH, the maximum downward fluxes are nearly coincident in the NH, and the minimum fluxes are offset by ~2 months. The downward mass flux begins to increase around June while the ozone flux is still decreasing. The ozone flux begins to increase in August. The ozone mixing ratio of the air subsiding across the 380 K surface during June and July decreases rapidly with time. The hemispheric difference of the ozone and mass flux phases illustrates that the seasonal cycles of the upper stratosphere wave-driven transport and chemistry have different phases in the NH and SH.

3.2. Tropopause Mass Flux

[18] The 380 K flux is diabatic by definition, but the transport across the tropopause can also occur adiabatically. The net, adiabatic, and diabatic extratropical cross-tropopause fluxes of mass and ozone are shown in Figure 2. The results for the individual stratospheric and tropospheric ozone fields are also displayed. The mass flux results generally agree with the FVGCM results of S04 (Figure 6 of S04). The minor differences are due to interannual variability. S04 shows only a single annual cycle, while a 5 year mean is presented here.

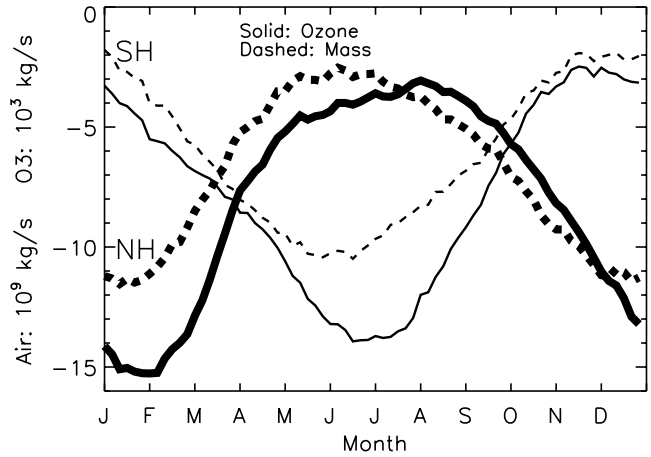

Figure 1. Annual cycle of the flux across the extratropical 380 K isentropic surface. Data are a 5 year mean. Bold (thin) lines are for the Northern (Southern) Hemisphere. Solid and dashed lines denote the ozone and mass fluxes, respectively. Note that the maximum downward flux occurs at the lowest point on each curve.

[19] Three day means of days 1, 5, and 10 and days 15, 20, and 25 of each month are used to generate Figure 2. The seasonal cycle of the net mass flux is less pronounced in the SH than in the NH (Figures 2a and 2b). This is primarily because the amplitude of the seasonal cycle of lowermost stratospheric mass (maximum to minimum differences) is smaller in the SH (not shown). However, the SH adiabatic and diabatic mass fluxes still exhibit strong seasonal cycles. In both hemispheres the rate of change of lowermost stratospheric mass is also responsible for the offset in the phase of the mass flux across the tropopause and 380 K surface (see equation (1)). The phase of the mass flux across the tropopause is predominately controlled by the seasonal vertical movement of the tropopause.

[20] The large adiabatic TST of mass that occurs throughout the year is in agreement with the findings of S04. This contrasts the STT result of *Dethof et al.* [2000] using contour advection to estimate the adiabatic mass flux across the tropopause on the 330, 345, and 360 K surfaces. This Eulerian result is compatible with the Lagrangian-based Dethof et al. method if a large amount of adiabatic TST occurs in the extratropics, poleward of where the 330 K surface intersects the tropopause or else in the tropics above 360 K. The present algorithm with a top boundary at 370 K or without the 30 g cm^{-2} minimum density criteria does not change the sign of the adiabatic TST (not shown). Thus there must be significant net adiabatic TST poleward of the 330 K tropopause boundary if the Lagrangian and Eulerian approaches are considered equivalent. This is consistent with the findings of *James et al.* [2003a] (also *Wernli and Bourqui* [2002]), who associate significant high-latitude TST with warm conveyor belts of blocking anticyclones.

3.3. Tropopause Ozone Flux

[21] In both hemispheres the variability of the adiabatic total ozone flux is much greater than the diabatic flux (Figures 2c and 2d). However, the magnitude of the diabatic flux is greater than the adiabatic flux through most of the year. Thus the magnitude of the annual total ozone flux is

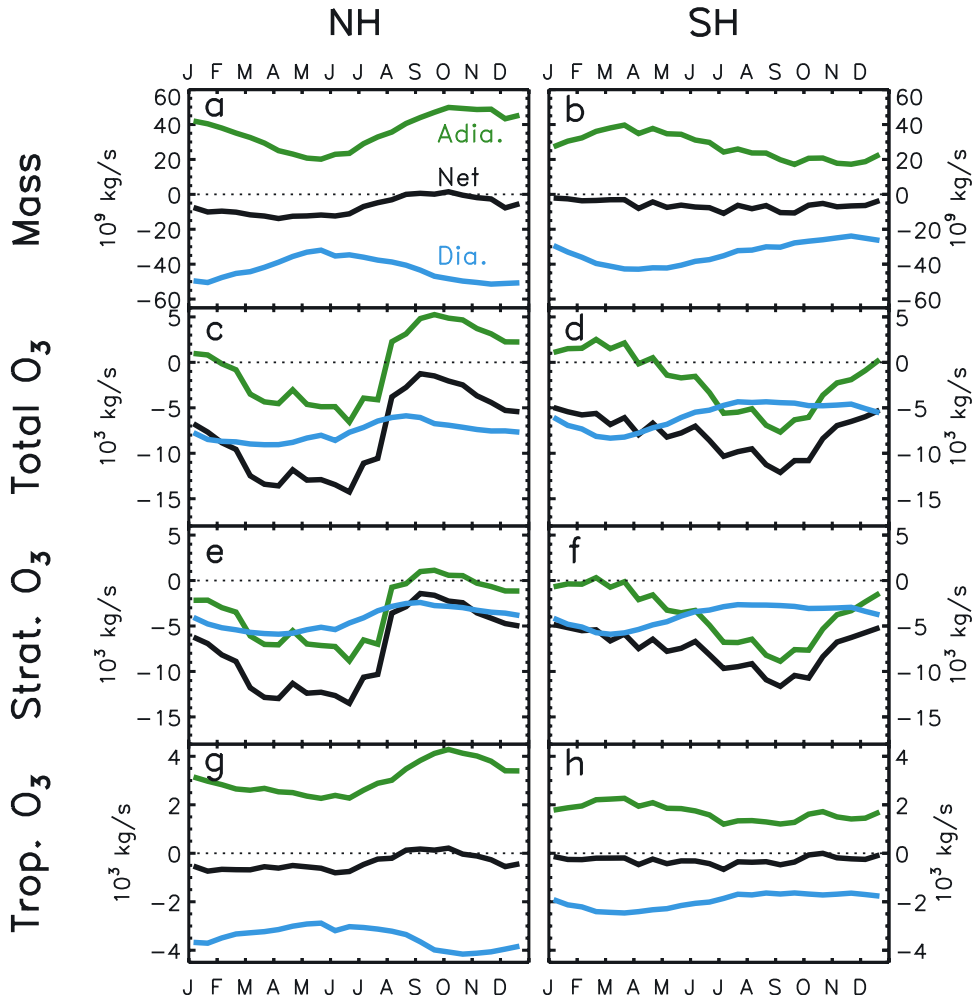

Figure 2. Annual mean cycles of net (black), adiabatic (green), and diabatic (blue) flux across the extratropical tropopause. Data are a 5 year mean. Positive flux is defined as TST, so the region above (below) the dashed zero flux line denotes TST (STT). Thus maximum STT occurs at the lowest point below the dashed line, and maximum TST occurs at the highest point above the dashed line. Left (right) column is the NH (SH) result. (a, b) Mass flux. (c, d) Total ozone (see text) flux. (e, f) Flux of ozone that was chemically produced in the stratosphere only. (g, h) Flux of ozone that was produced in the troposphere. Note the different scales used for mass and ozone.

dominated by the diabatic component; the seasonality of the flux is controlled by the isentropic component. In addition, the seasonal cycle of the net ozone transport across the tropopause is similar to that of the mass flux, and the adiabatic mass and ozone fluxes also have a similar phase. However, there is a phase difference between the diabatic components of the ozone flux and mass flux.

[22] Perhaps the most noticeable difference between the total ozone and mass fluxes in Figures 2a–2d is that the adiabatic flux of ozone is from the stratosphere to the troposphere for about half of the year in both hemispheres, while the net mass transport is consistently from the troposphere to the stratosphere. This is a consequence of the strong vertical gradient of ozone near the tropopause. Adiabatic STT (TST) results in mixing ratios at the local tropopause that are relatively large (small). The ozone mixing ratio field at the tropopause is correlated with the direction of isentropic transport through the surface. Areas of abnormally high (low) ozone mixing ratio at the tropopause at a given time may indicate active or recent STT (TST).

[23] The seasonal variability of the mean ozone mixing ratio at the tropopause can be surmised from comparing the annual cycles of ozone and mass flux. The downward adiabatic flux of ozone decreases more rapidly than the mass around July and August in the NH and October and November in the SH. Furthermore, the minimum downward flux of ozone leads the mass flux by ~1 month. The mean ozone mixing ratio at the tropopause where the majority of the flux occurs rapidly decreases during this time and then begins to increase again before the downward mass flux has reached a minimum. The diabatic fluxes are even more out of phase, especially in the NH. The phase differences that exist between the adiabatic and diabatic components imply that the cross-tropopause transport pathways are primarily either adiabatic or diabatic. The adiabatic and diabatic seasonal cycles would have similar phases if many of the transport pathways were the result of adiabatic and diabatic

Table 1. Annual STE of Mass[a]

Tropopause Mass Flux	This Study 5 Year Mean (Range)	S04 (FVGCM) 1 year	A96 2 Year Mean	*Dethof et al.* [2000] 2 Year Mean NH/1 Year SH	*Seo and Bowman* [2002] 2 Year Mean	*James et al.* [2003a] 15 Year Mean
Net NH	−2.2 (−2.1 to −2.3)	−2.3	−3.5		−3.7	−4.1
Net SH	−1.9 (−1.8 to −2.1)	−1.8	−3.3		−3.2	−3.5
Adiabatic NH	11.4 (10.9 to 11.9)	11.7		−11.0		
Adiabatic SH	8.7 (8.4 to 8.9)	8.5		−14.5		
Diabatic NH	−13.6 (−13.1 to −14.1)	−13.9				
Diabatic SH	−10.6 (−10.2 to −11.0)	−10.1				

[a]Ranges given are from the five annual totals. Values are given in 10^{17} kg yr^{-1}.

processes acting concurrently and in tandem. In other words, if the majority of the grid points where STE occurred exhibited both adiabatic and diabatic flux of comparable magnitude, the adiabatic and diabatic ozone flux seasonal phases would be similar since the air transported would have the same ozone mixing ratio.

[24] The net total ozone flux across the tropopause is clearly dominated by the stratospheric ozone (Figures 2e–2h). The net stratospheric ozone flux is nearly an order of magnitude greater than the net tropospheric ozone flux, and it also exhibits greater seasonal variability. The tropospheric ozone component modulates the total ozone flux to a limited degree. The most notable difference between the stratospheric and tropospheric ozone fluxes is that the tropospheric component most resembles the mass flux. The adiabatic tropospheric ozone flux is always directed into the stratosphere, and the seasonal cycle is almost identical to the mass flux. Three factors contribute to the similarity of the tropospheric ozone and mass fluxes: (1) above the upper troposphere the tropospheric ozone decreases with altitude similar to mass, (2) the vertical gradient of tropospheric ozone across the tropopause is not as great as the stratospheric ozone, and (3) the seasonal and spatial variability of tropospheric ozone at the tropopause is much smaller than the stratospheric component.

4. Discussion

[25] Table 1 presents the net annual mass transport across the tropopause along with results from other selected studies for comparison. Note that the calculated net annual transport across the extratropical 380 K surface is the same as the calculated net annual tropopause flux given in Table 1. The mass fluxes of the present study are very similar to the FVGCM S04 results since the same diagnostic algorithm and core GCM were used. This illustrates that the use of 6 days per month is adequate to estimate the annual flux and represent the seasonal cycles.

[26] The net mass flux results here range from 30 to 40% less than those of other studies shown in Table 1. These other studies share the trait that the meteorological fields used are from assimilation systems, contrasting the GCM fields used here. Assimilation systems tend to have too strong of a residual circulation, and the age of air is too young compared to observations. This is most likely to affect the studies that diagnose STE in a Lagrangian framework. A more detailed discussion of the bias introduced by model or assimilation system may be found in S04.

[27] *Dethof et al.* [2000] show an annual STT adiabatic flux with only a couple of months that exhibit TST. This contrasts with the results of S04 and this study that show persistent adiabatic TST. As discussed in section 3, this discrepancy implies that there is a relatively large adiabatic flux of air directed into the lower stratosphere poleward of the tropopause 330 K boundary. *James et al.* [2003a] use a Lagrangian particle dispersion model to find that significant TST of net mass occurs poleward of ~51° latitude, however, they do not differentiate between adiabatic and diabatic fluxes. The present study suggests that the bulk of the high-latitude TST is isentropic.

[28] The annual transport of total ozone across the extratropical tropopause agrees well with both empirical- and model-based estimates of other recent studies (Table 2). The most notable difference is that the net flux of total ozone in the SH of the present work is nearly the same as in the NH. While the net mass flux in the NH is 15% greater than the SH, the CTM mean ozone mixing ratio at the tropopause is greater in the SH. This is a result of two factors: (1) the ozone mixing ratio in the SH midlatitude lowermost stratosphere is biased ~10% high with respect to observations as discussed in section 2, and (2) the stratospheric chlorine burden and other ozone-depleting chemical species correspond to the years 1979–1983 in the CTM output used in this study. Thus the chemical depletion of ozone in the stratosphere is significantly less than present-day, particularly in the SH polar vortex.

[29] *Jing et al.* [2004] apply PV ozone mapping to the same contour advection method used by *Dethof et al.* [2000] to investigate the isentropic cross-tropopause trans-

Table 2. Annual STE of Total Ozone[a]

Tropopause Total Ozone Flux	This Study 5 Year Mean (Range)	*Olsen et al.* [2003] (30°–60°) 1 Year	*Gettelman et al.* [1997] 4 Year Mean	*McLinden et al.* [2000] (Linoz) 1 Year	*Jing et al.* [2004] 1 Year
Net NH	−252 (−239 to −273)	−260	−290	−198 to −412	
Net SH	−248 (−240 to −250)	−210	−220	−175 to −378	
Adiabatic NH	−10 (−2 to −17)				−46
Adiabatic SH	−64 (−55 to −72)				
Diabatic NH	−243 (−230 to −261)				
Diabatic SH	−183 (−175 to −194)				

[a]Ranges given are from the five annual totals. Values are given in Tg yr^{-1}.

Table 3. Annual STE of Stratospheric and Tropospheric Ozone[a]

Tropopause Ozone Component Flux	Adiabatic Stratospheric Ozone	Diabatic Stratospheric Ozone	Adiabatic Tropospheric Ozone	Diabatic Tropospheric Ozone
NH	−107	−133	97	−110
SH	−117	−122	53	−62

[a]Values are given in Tg yr^{-1}.

port of ozone. They find that the maximum net downward flux of ozone occurs in the summer months in agreement with the results shown in Figure 2c. However, in the *Jing et al.* study the rapid decrease in the magnitude of the net downward flux in the late summer shown here is not evident. In addition, the net adiabatic flux is not directed into the stratosphere during the late summer and fall as in the present study. Jing et al. follow the method of Dethof et al. and primarily examine the exchange between the mid-latitude stratosphere and tropical troposphere. The lowest isentropic surface that is considered is 335 K. The differences between the seasonal cycles of the adiabatic ozone flux are likely attributable to transport at higher latitudes.

[30] The SH adiabatic ozone flux magnitude is 6 times greater than the NH (Table 2) even though the NH adiabatic mass flux is greater than the SH (Table 1). This is in contrast to the NH/SH ratio of the diabatic mass flux being nearly equal to the NH/SH ratio of the diabatic ozone flux. The cause of the adiabatic disparity is found by examining the fluxes of tropospheric ozone and stratospheric ozone separately (Table 3). The NH adiabatic tropospheric ozone TST is almost twice as great as in the SH. The NH and SH adiabatic stratospheric ozone STT fluxes are within ~10% of each other. Thus the NH adiabatic total ozone STT is much less due to the large adiabatic TST of tropospheric ozone (that returns to the troposphere diabatically). This is consistent with observations that the NH troposphere has a greater burden of ozone than the SH [*Fishman et al.*, 1990; *Logan*, 1999].

[31] The diabatic fluxes of mass across the tropopause in the NH and SH are temporally out of phase as expected (Figures 2a–2b). However, the hemispheric diabatic ozone fluxes are nearly in phase (Figures 2c–2d). This implies that the CTM annual cycles of mean ozone mixing ratios at the tropopause are not similar with respect to the NH and SH season. Figure 3a shows the zonal diabatic flux of mass across the tropopause for the months of March and September. These months correspond to the times of maximum and minimum diabatic ozone flux. The maximum downward mass flux is shifted toward the pole (equator) in the fall (spring) in both hemispheres. However, the zonal mean ozone mixing ratio at the tropopause poleward of ~45° is greater in March of both hemispheres (Figure 3b). This seasonal cycle of CTM ozone agrees well with observations (Figure 4). Figure 4a shows the annual cycle of mean daily ozonesonde observations on the 240 hPa surface for middle and high latitudes in the NH and SH. The NH observations exhibit relatively little phase shift between the middle and high latitudes. In contrast, the middle- and high-latitude annual cycles are nearly a half year out of phase in the SH. This shift is seen at all lowermost stratosphere pressures. For comparison the seasonal cycles of CTM total ozone mixing ratio at the tropopause over the same latitude bands are shown in Figure 4b. A similar phase shift between the SH middle- and high-latitude CTM total ozone mixing ratio exists, in agreement with the ozonesonde data. The CTM tropospheric ozone fields do not exhibit this shift with latitude. It is unlikely that ozone depletion in the Antarctic ozone hole is the primary cause of this shift since the mean mixing ratio at the polar latitudes begins decreasing about April. It is possible that the stratospheric polar vortex blocks meridional transport more effectively in the SH, resulting in this latitudinal shift in the annual cycle of ozone mixing ratio. This is likely due to the greater depth and persistence of the SH vortex [*Manney and Zurek*, 1993].

[32] The magnitudes of the adiabatic and diabatic fluxes of the tropospheric and stratospheric ozone are of the same order. However, Figures 2e–2h and Table 3 show that the net stratospheric ozone flux is an order of magnitude greater

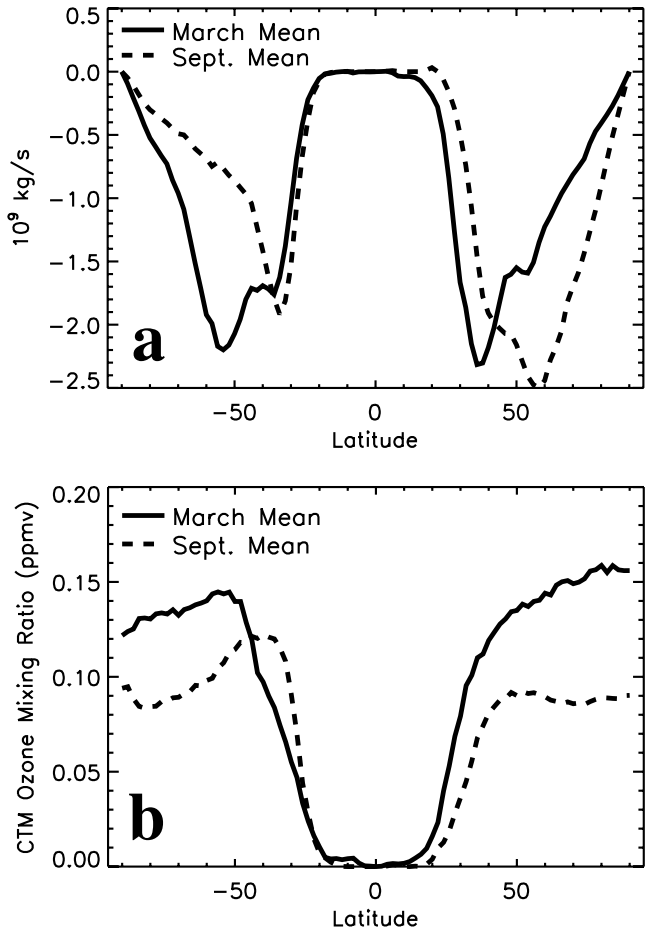

Figure 3. (a) Diabatic mass flux across the extratropical tropopause by latitude for the months of March (solid) and September (dashed). Note the vertical axis follows the convention of previous figures that the maximum flux from the stratosphere to the troposphere is the lowest point of each curve. (b) Mean total ozone mixing ratio at the extratropical tropopause by latitude for the months of March (solid) and September (dashed). Note that the flux and mixing ratio are set to zero at grid cells considered tropical by using the 30 g cm^{-2} lowermost stratosphere cutoff criteria.

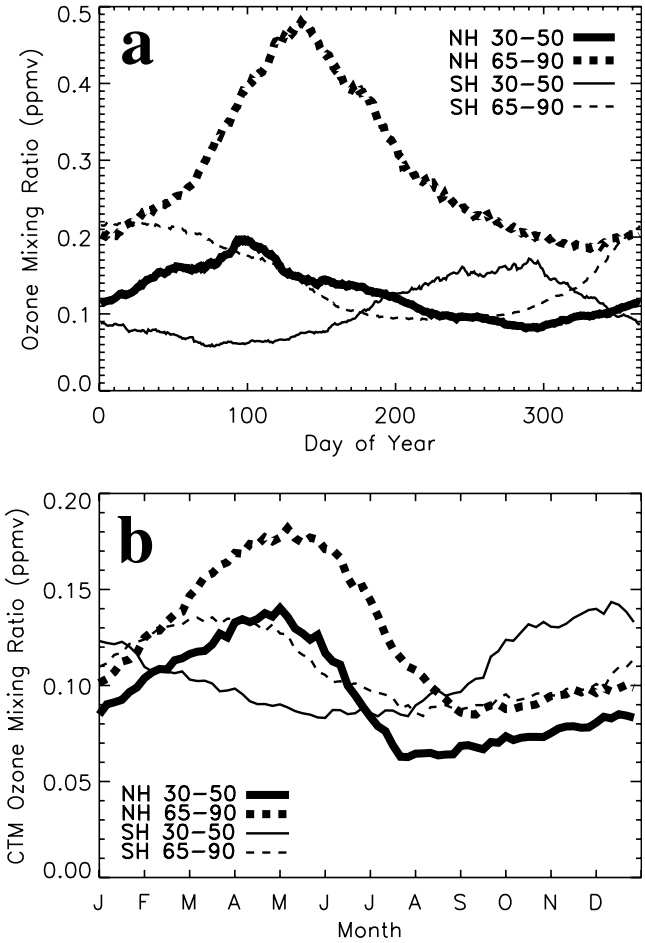

Figure 4. (a) Ozonesonde observations on the 240 hPa surface within the specified latitude bands. Data are equal-weighted averages of the sondes in each latitude band from 1988 to 2002. The 30°–50° latitude band includes seven and two ozonesonde stations in the NH (bold solid) and SH (thin solid), respectively. Both the NH and SH polar regions (bold dashed and thin dashed, respectively) include four stations. (b) Mean CTM total ozone mixing ratio at the tropopause within the specified latitude bands. Note that the ozonesonde observations are on the 240 hPa surface and the CTM ozone is at the tropopause; thus the magnitudes are not similar. Phases are the relevant points discussed in the text.

than the net tropospheric ozone flux in each hemisphere. This is a result of the oppositely directed adiabatic tropospheric ozone transport. Any STT event, particularly the diabatic events, may contain a significant fraction of ozone that is not of stratospheric origin. This underscores the need for additional tracer information in any ozone STT estimate derived from measurements if the amount of stratospheric origin ozone is desired.

[33] The diagnostic algorithm does not provide any specific spatial information of the net and adiabatic transport. In contrast, the spatial distribution of the diabatic flux is explicitly determined by the heating rates at the tropopause. The global distributions of the diabatic mass and ozone fluxes averaged over the entire 5 year period are shown in Figure 5a. The majority of the flux occurs in the midlatitudes between 30° and 60° in both hemispheres. The strongest transport in the NH is associated with climatological storm tracks in the northern Pacific and Atlantic oceans. This spatial distribution of diabatic flux is consistent with the STT results of *Sprenger and Wernli* [2003]. In addition, *Sprenger and Wernli* show that the greatest TST occurs at higher latitudes, which is consistent with the inferred adiabatic flux of the present study. In the SH the greatest diabatic flux regions are shifted toward the equator. It is also noted that there is less diabatic flux over the Himalaya, Rocky, and Andes Mountains compared to adjacent areas. The colder tropopause temperatures above the higher surface elevations are closer to radiative equilibrium, and the diabatic descent is reduced.

[34] The relatively zonal diabatic mass flux distribution corresponds well with the ozone flux in the 5 year mean (Figure 5a). Figure 5b shows the instantaneous diabatic ozone and mass fluxes on a single February day. Only a portion of the NH is shown to facilitate viewing the fine-scale detail. The instantaneous ozone and mass flux fields are less consistent compared to the 5 year mean fields of Figure 5a. These differences must be due to the spatial variability of the ozone mixing ratio at the tropopause since the ozone flux is derived directly from the mass flux. This

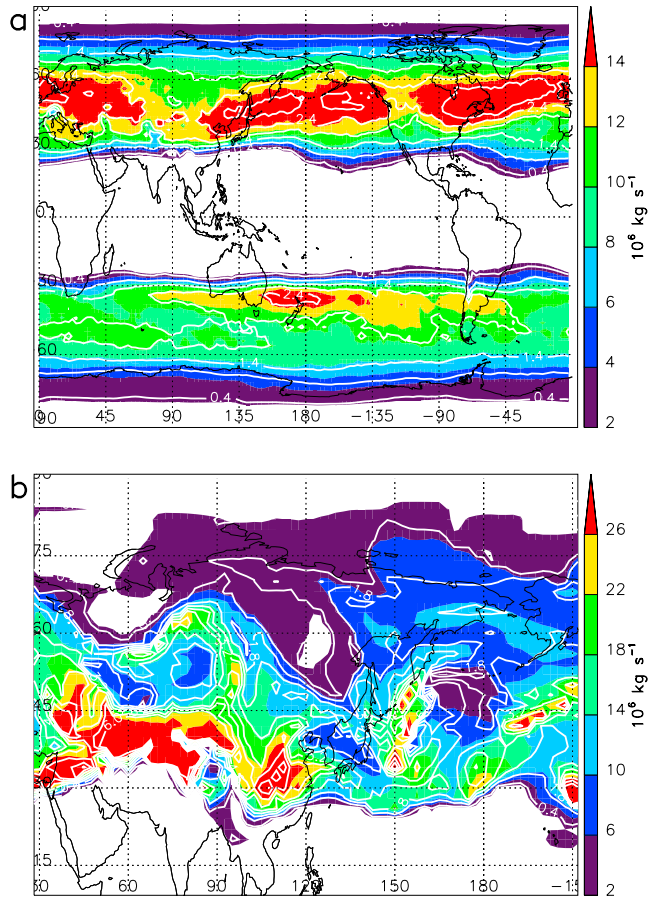

Figure 5. (a) Five year mean diabatic flux of mass (color shading) and ozone (white contours). Ozone flux contour interval is 0.5 kg s^{-1} beginning at 0.4 kg s^{-1}. (b) Mean diabatic mass flux on a single February day. Ozone flux contour interval is 0.7 kg s^{-1} beginning at 0.4 kg s^{-1}.

illustrates the significant error that may be introduced when estimating ozone transport by simplified calculations such as applying a mean mixing ratio of ozone to a calculated mass flux. However, the agreement between the 5 year mean fields shows that this error is minimal when the latitudinal dependency of ozone mixing ratio and sufficiently long timescales are considered.

[35] The diabatic fluxes of mass, tropospheric ozone, and stratospheric ozone exhibit much less short timescale variability than the respective adiabatic fluxes (not shown since the short timescales are smoothed in Figure 2). This indicates that the adiabatic exchange is more episodic and event driven than the diabatic transport. Figure 5 illustrates that the diabatic exchange is dominated by persistent, midlatitude descent but is modulated by episodic events. These events, such as baroclinic cyclones, tend to temporarily and locally "redistribute" the diabatic mass and ozone flux, but they do not significantly alter the hemispheric totals of these on daily timescales.

[36] As discussed in section 3.2, significant adiabatic TST occurs at high latitudes. The net adiabatic transport of both tropospheric ozone and mass is directed into the stratosphere throughout the annual cycle. Figure 5 shows that the diabatic STT is concentrated at midlatitudes. This implies that there is a net mean meridional circulation with diabatic STT at midlatitudes and adiabatic TST at higher latitudes. The maximum adiabatic TST of mass occurs in the autumn of each hemisphere, corresponding to the movement of the tropopause moving downward relative to the potential temperature field. *James et al.* [2003b] show that "shallow" STT frequently is a transient flux; the mass reenters the stratosphere over short timescales on the order of a day. This rapid transient transport is a problem for many flux estimates since the net flux is a residual of large upward and downward terms. This mean meridional circulation of STT-TST in the present study, in which the troposphere-to-stratosphere transition is due primarily to the downward movement of the tropopause rather than the transport of the air parcels, is likely a longer timescale process than discussed by *James et al.* [2003b].

5. Summary and Conclusion

[37] The diagnostic algorithm introduced by A96 and extended by S04 has been used to estimate the adiabatic and diabatic transport of mass and ozone across the extratropical tropopause. The mass and ozone fluxes exhibit slightly different seasonal cycles with a phase offset on the order of a couple months. This is most evident comparing the flux across the 380 K surface. This is caused by the seasonal cycle of ozone at 380 K being out of phase with the transport seasonal cycle.

[38] The algorithm used here provides only a bulk estimate of the adiabatic exchange, though much can be inferred from the spatial information of the diabatic transport and the diagnosed ozone flux. The net adiabatic (diabatic) mass flux is directed into the stratosphere (troposphere) throughout an annual cycle. Thus the isentropic transport through tropopause folds, across the subtropical jet, and by other means contributes relatively little to the net mass STT compared to diabatic mechanisms. The net adiabatic TST of mass is primarily due to a large flux at high latitudes. A mean meridional circulation consisting of adiabatic TST at higher latitudes and diabatic STT at midlatitudes is indicated by the fluxes of mass and ozone. This is likely a longer timescale transient flux than previously investigated [*Wernli and Bourqui*, 2002; *James et al.*, 2003b; *Stohl et al.*, 2003b]. In addition, differences between the adiabatic and diabatic ozone fluxes suggest that the pathways of cross-tropopause transport are generally distinct. At least the majority of the pathways can be characterized as being either dominantly adiabatic or diabatic. The pathways are less likely to result from adiabatic and diabatic processes acting concurrently on the same air parcel.

[39] The annual cycle of the adiabatic transport has more long and short timescale variability than the diabatic flux. Thus the seasonal and daily variability of the net mass and ozone flux is dominated by the adiabatic transport. The NH and SH diabatic fluxes of stratospheric ozone across the tropopause are nearly in phase. This contrasts the diabatic mass and tropospheric ozone fluxes that are a half year out of phase as expected from seasonal arguments. The SH seasonal cycle of higher-latitude ozone at the tropopause is shifted nearly a half year out of phase with respect to the lower latitude seasonal cycle. This is caused by blocking of meridional transport by the SH polar vortex.

[40] This study shows that significant error may be introduced when estimating an ozone flux by applying a simple, large-scale mean ozone mixing ratio to a mass flux. However, the error is minimal if seasonal or annual timescales are considered. Comparison of the diabatic fluxes of mass and ozone show that there is significant daily spatial variability of ozone mixing ratio at the tropopause. In addition, the net adiabatic flux of ozone is in the opposite direction to the mass flux through much of an annual cycle. This implies that the ozone mixing ratio at the tropopause is anomalously high where STT occurs and/or anomalously low where TST occurs. The tropopause ozone mixing ratio acts as a recorder of the direction of transport through the surface, at least for short durations. Furthermore, any ozone STT derived from measurements may include a substantial amount of tropospheric origin ozone. This is particularly true in the case of diabatic STT.

[41] **Acknowledgments.** The authors are grateful to Gordon Labow for providing the ozonesonde data. NASA's EOS IDS and ACMAP programs supported this work.

References

Appenzeller, C., J. R. Holton, and K. H. Rosenlof (1996), Seasonal variation of mass transport across the tropopause, *J. Geophys. Res.*, *101*, 15,071–15,078.

Beekmann, M., et al. (1997), Regional and global tropopause fold occurrence and related ozone flux across the tropopause, *J. Atmos. Chem.*, *28*, 29–44.

Bey, I., D. J. Jacob, R. M. Yantosca, J. A. Logan, B. Field, A. M. Fiore, Q. Li, H. Liu, L. J. Mickley, and M. Schultz (2001), Global modeling of tropospheric chemistry with assimilated meteorology: Model description and evaluation, *J. Geophys. Res.*, *106*, 23,073–23,096.

Brewer, A. M. (1949), Evidence for a world circulation provided by the measurements of helium and water vapor distribution in the stratosphere, *Q. J. R. Meteorol. Soc.*, *75*, 351–363.

Dethof, A., A. O'Neill, and J. Slingo (2000), Quantification of the isentropic mass transport across the dynamical tropopause, *J. Geophys. Res.*, *105*, 12,279–12,293.

Dobson, G. M. B. (1956), Origin and distribution of polyatomic molecules in the atmosphere, *Proc. R. Soc. London, Ser. A*, *236*, 187–193.

Douglass, A. R., M. R. Schoeberl, R. B. Rood, and S. Pawson (2003), Evaluation of transport in the lower tropical stratosphere in a global

chemistry and transport model, *J. Geophys. Res.*, *108*(D9), 4259, doi:10.1029/2002JD002696.
Fishman, J., C. E. Watson, J. C. Larsen, and J. A. Logan (1990), The distribution of tropospheric ozone obtained from satellite data, *J. Geophys. Res.*, *95*, 3599–3617.
Fleming, E. L., C. H. Jackman, J. E. Rosenfield, and D. B. Considine (2002), Two-dimensional model simulations of the QBO in ozone and tracers in the tropical stratosphere, *J. Geophys. Res.*, *107*(D23), 4665, doi:10.1029/2001JD001146.
Garcia, R. R., and B. A. Boville (1994), Downward control of the mean meridional circulation and temperature distribution of the polar winter stratosphere, *J. Atmos. Sci.*, *51*, 2238–2245.
Gettelman, A., J. R. Holton, and K. H. Rosenlof (1997), Mass fluxes of O_3, CH_4, N_2O, and CF_2Cl_2 in the lower stratosphere calculated from observational data, *J. Geophys. Res.*, *102*, 19,149–19,159.
Hauglustaine, D. A., G. P. Brasseur, S. Walters, P. J. Rasch, J.-F. Müller, L. K. Emmons, and M. A. Carroll (1998), MOZART, a global chemical transport model for ozone and related chemical tracers: 2. Model results and evaluation, *J. Geophys. Res.*, *103*, 28,291–28,335.
Haynes, P. H., M. E. McIntyre, T. G. Sheperd, C. J. Marks, and K. P. Shine (1991), On the "downward control" principle of extratropical circulations by eddy-induced mean zonal forces, *J. Atmos. Sci.*, *48*, 651–678.
Hoerling, M. P., T. K. Schaack, and A. J. Lenzen (1991), Global objective tropopause analysis, *Mon. Weather Rev.*, *119*, 1816–1831.
Holton, J. R., P. H. Haynes, M. E. McIntyre, A. R. Douglass, R. B. Rood, and L. Pfister (1995), Stratosphere-troposphere exchange, *Rev. Geophys.*, *33*, 403–439.
Hoskins, B. J. (1991), Toward a PV-theta view of the general circulation, *Tellus, Ser. A*, *43*, 27–35.
James, P., A. Stohl, C. Forster, S. Eckhardt, P. Seibert, and A. Frank (2003a), A 15-year climatology of stratosphere-troposphere exchange with a Lagrangian particle dispersion model: 1. Methodology and validation, *J. Geophys. Res.*, *108*(D12), 8519, doi:10.1029/2002JD002637.
James, P., A. Stohl, C. Forster, S. Eckhardt, P. Seibert, and A. Frank (2003b), A 15-year climatology of stratosphere-troposphere exchange with a Lagrangian particle dispersion model: 2. Mean climate and seasonal variability, *J. Geophys. Res.*, *108*(D12), 8522, doi:10.1029/2002JD002639.
Jing, P., D. M. Cunnold, H. J. Wang, and E.-S. Yang (2004), Isentropic cross-tropopause ozone transport in the Northern Hemisphere, *J. Atmos. Sci.*, *61*, 1068–1078.
Kiehl, J. T., J. J. Hack, G. B. Bonan, B. A. Boville, D. L. Williamson, and P. J. Rasch (1998), The National Center for Atmospheric Research Community Climate Model: CCM3, *J. Clim.*, *11*(6), 1131–1149.
Lamarque, J.-F., and P. G. Hess (1994), Cross-tropopause mass exchange and potential vorticity budget in a simulated tropopause folding, *J. Atmos. Sci.*, *51*, 2246–2269.
Lamarque, J. F., P. G. Hess, and X. X. Tie (1999), Three-dimensional model study of the influence of stratosphere-troposphere exchange and its distribution on tropospheric chemistry, *J. Geophys. Res.*, *104*, 26,363–26,372.
Levy, H., II (1971), Normal atmosphere: Large radical and formaldehyde concentrations predicted, *Science*, *173*, 141–143.
Lin, S. J. (1997), A finite-volume integration scheme for computing pressure-gradient forces in general vertical coordinates, *Q. J. R. Meteorol. Soc.*, *123*, 1749–1762.
Lin, S. J., and R. B. Rood (1996), Multidimensional flux-form semi-Lagrangian transport schemes, *Mon. Weather Rev.*, *124*, 2046–2070.
Lin, S. J., and R. B. Rood (1997), An explicit flux-form semi-Lagrangian shallow-water model on the sphere, *Q. J. R. Meteorol. Soc.*, *124*, 2477–2498.
Logan, J. A. (1999), An analysis of ozonesonde data for the troposphere: Recommendations for testing 3-D models and development of a gridded climatology for tropospheric ozone, *J. Geophys. Res.*, *104*, 16,115–16,149.
Manney, G. L., and R. W. Zurek (1993), Interhemispheric comparison of the development of the stratospheric polar vortex during fall: A 3-dimensional perspective for 1991–1992, *Geophys. Res. Lett.*, *20*(12), 1275–1278.
Matsumoto, S., K. Ninomiya, R. Hasegawa, and Y. Miki (1982), The structure and role of subsynoptic scale cold vortex on the heavy precipitation, *J. Meteorol. Soc. Jpn.*, *90*(D2), 339–353.
McLinden, C. A., S. C. Olsen, B. Hannegan, O. Wild, M. J. Prather, and J. Sundet (2000), Stratospheric ozone in 3-D models: A simple chemistry and the cross-tropopause flux, *J. Geophys. Res.*, *105*, 14,653–14,665.
Murphy, D. M., and D. W. Fahey (1994), An estimate of the flux of stratospheric reactive nitrogen and ozone into the troposphere, *J. Geophys. Res.*, *99*, 5325–5332.
Norton, W. A. (1994), Breaking Rossby waves in a model stratosphere diagnosed by a vortex following coordinate system and a technique for advecting material contours, *J. Atmos. Sci.*, *51*, 654–673.
Olsen, M. A., and J. L. Stanford (2001), Evidence of stratosphere-to-troposphere transport within a mesoscale model and Total Ozone Mapping Spectrometer total ozone, *J. Geophys. Res.*, *106*, 27,323–27,334.
Olsen, M. A., A. R. Douglass, and M. R. Schoeberl (2003), A comparison of Northern and Southern Hemisphere cross-tropopause ozone flux, *Geophys. Res. Lett.*, *30*(7), 1412, doi:10.1029/2002GL016538.
Ramanathan, V., et al. (1987), Climate-chemical interactions and effects of changing atmospheric trace gases, *Rev. Geophys.*, *25*, 1441–1482.
Reed, R. J., and F. Sanders (1953), An investigation of the development of a mid-tropospheric frontal zone and its associated vorticity field, *J. Meteorol.*, *10*, 338–349.
Roelofs, G.-J., and J. Lelieveld (1995), Distribution and budget of O_3 in the troposphere calculated with a chemistry general circulation model, *J. Geophys. Res.*, *100*, 20,983–20,998.
Roelofs, G.-J., J. Lelieveld, and R. van Dorland (1997), A three-dimensional chemistry/general circulation model simulation of anthropogenically derived ozone in the troposphere and its radiative climate forcing, *J. Geophys. Res.*, *102*, 23,389–23,401.
Roelofs, G. J., et al. (2003), Intercomparison of tropospheric ozone models: Ozone transport in a complex tropopause folding event, *J. Geophys. Res.*, *108*(D12), 8529, doi:10.1029/2003JD003462.
Rood, R. B., A. R. Douglass, M. C. Cerniglia, and W. G. Read (1997), Synoptic-scale mass exchange from the troposphere to the stratosphere, *J. Geophys. Res.*, *102*, 23,467–23,485.
Schoeberl, M. R. (2004), Extratropical stratosphere-troposphere mass exchange, *J. Geophys. Res.*, *109*, D13303, doi:10.1029/2004JD004525.
Schoeberl, M. R., A. R. Douglass, Z. Zhu, and S. Pawson (2003), A comparison of the lower stratospheric age spectra derived from a general circulation model and two data assimilation systems, *J. Geophys. Res.*, *108*(D3), 4113, doi:10.1029/2002JD002652.
Seo, K. H., and K. P. Bowman (2002), Lagrangian estimate of global stratosphere-troposphere mass exchange, *J. Geophys. Res.*, *107*(D21), 4555, doi:10.1029/2002JD002441.
Sprenger, M., and H. Wernli (2003), A Northern Hemispheric climatology of cross-tropopause exchange for the ERA15 time period (1979–1993), *J. Geophys. Res.*, *108*(D12), 8521, doi:10.1029/2002JD002636.
Staley, D. O. (1962), On the mechanism of mass and radioactivity transport from the stratosphere to the troposphere, *J. Atmos. Sci.*, *19*, 450–467.
Stohl, A., et al. (2003a), Stratosphere-troposphere exchange: A review, and what we have learned from STACCATO, *J. Geophys. Res.*, *108*(D12), 8516, doi:10.1029/2002JD002490.
Stohl, A., H. Wernli, P. James, M. Bourqui, C. Forster, M. A. Liniger, P. Seibert, and M. Sprenger (2003b), A new perspective of stratosphere-troposphere exchange, *Bull. Am. Meteorol. Soc.*, *84*, 1565–1573.
Tie, X.-X., and P. Hess (1997), Ozone mass exchange between the stratosphere and troposphere for background and volcanic sulfate aerosol conditions, *J. Geophys. Res.*, *102*, 25,487–25,500.
Waugh, D. W., and R. A. Plumb (1994), Contour advection with surgery: A technique for investigating finescale structure in tracer transport, *J. Atmos. Sci.*, *51*, 530–540.
Wernli, H., and M. Bourqui (2002), A Lagrangian "1-year climatology" of (deep) cross-tropopause exchange in the extratropical Northern Hemisphere, *J. Geophys. Res.*, *107*(D2), 4021, doi:10.1029/2001JD000812.
World Meteorological Organization (1986), Atmospheric ozone 1985: Global ozone research and monitoring report, *Rep. 16*, 392 pp., World Meteorol. Organ., Geneva, Switzerland.
World Meteorological Organization (2003), Scientific assessment of ozone depletion: 2002, global ozone research and monitoring project, *Rep. 47*, 498 pp., World Meteorol. Organ., Geneva, Switzerland.

A. R. Douglass and M. R. Schoeberl, NASA Goddard Space Flight Center, Code 916, Bldg. 33, Rm. E323, Greenbelt, MD 20771-0001, USA.
M. A. Olsen, NASA Goddard Space Flight Center, Code 916, Greenbelt, MD 20771-001, USA. (olsen@hyperion.gsfc.nasa.gov)